# Air Film System for Handling Semiconductor Wafers

In an automated fabrication facility, the thin, fragile silicon wafers in which semiconductor circuits are formed must be transported to and from processing stations with a minimum of contact with other solid objects so as to minimize damage, contamination, and consequent lowering of product yield. This task has been undertaken for some time now, in IBM and elsewhere, by systems based on a lubricating film of air as a means for levitating and moving wafers. However, due to inherent motion instabilities and specific control needs, some solid contact is typically involved in effecting prescribed wafer motion. The need for solid contact control is greatly reduced by the air film system described in this paper. It is based on a surface configuration that combines two fluid mechanics phenomena to generate a supporting air film that provides and guides wafer motion. Wafer transportation and positioning are achieved with the air film operating in conjunction with special control device techniques.

#### Introduction

The production of electronic modular circuits in thin and fragile silicon wafers involves a variety of complex processing steps. These operations require considerable handling of the wafers, which must be done in a way that minimizes damage and contamination and thus avoids lowering of product yield. The processor stations in such a facility are all connected to an atmospherically controlled wafer delivery apparatus that performs the functions illustrated in Fig. 1. The wafer transport apparatus must provide-with a minimum of contact with other solid objects—a rapid, secure, clean, and dependable delivery of wafers to the stations. Because of the extent, configuration, and requirements of the system, various difficult motion control functions are involved. Not only must the apparatus transport wafers over different distances, but it must also have means for stopping, positioning, redirecting, and providing other specific motions.

For some time now, in IBM and elsewhere, wafers have been moved on a lubricating film of air in an effort to minimize physical contact. Generally speaking, the implementation of this idea entails the use of flat perforated surfaces through which a continuous supply of air under

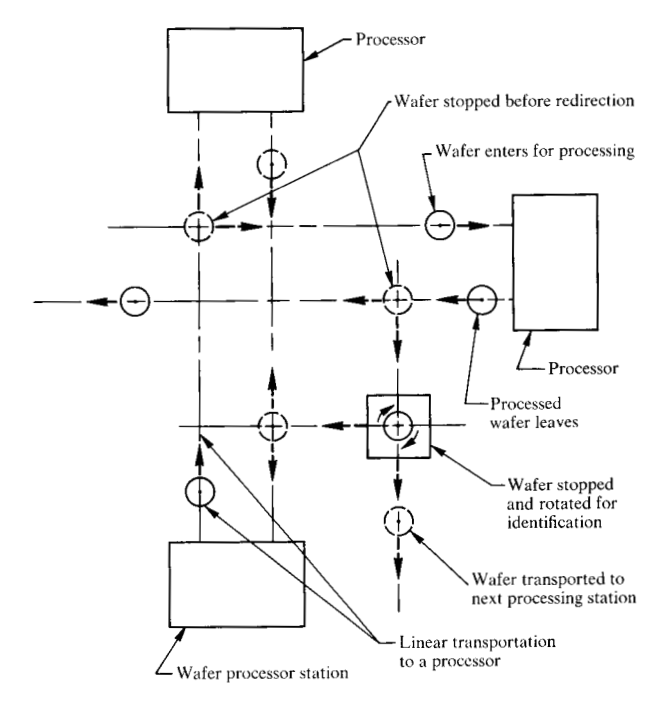
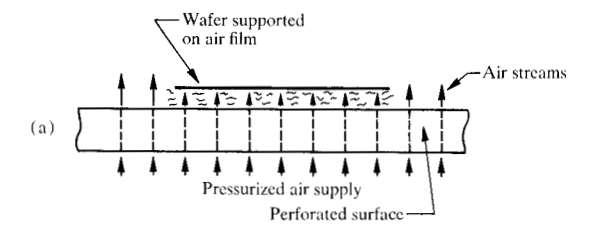
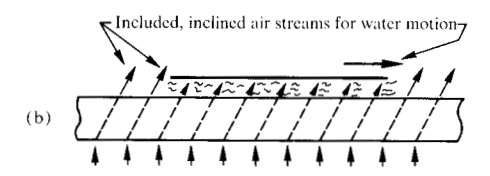


Figure 1 Typical motion control functions of a wafer delivery apparatus.

Copyright 1979 by International Business Machines Corporation. Copying is permitted without payment of royalty provided that (1) each reproduction is done without alteration and (2) the *Journal* reference and IBM copyright notice are included on the first page. The title and abstract may be used without further permission in computer-based and other information-service systems. Permission to *republish* other excerpts should be obtained from the Editor.





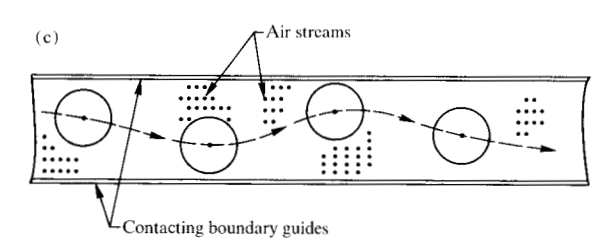


Figure 2 Wafer levitation (a), movement on an air film (b), and constrained linear motion (c).

pressure is forced (see Fig. 2). These surfaces are either of a porous sintered material or a material containing an array of small holes. When a wafer is placed over the air streams issuing from the surface, a cushioning air film is formed which supports it. The wafer is moved and maneuvered by the impulse action of air streams issuing from appropriately oriented openings. In addition, to constrain wafer motion in a prescribed manner, various forms of solid contacting means are typically required. For example, in linear transportation over a distance, the effects of low sliding friction and momentum of the moving wafer cause it to diverge from the desired direction. Consequently, as illustrated in Fig. 2, contacting boundary guides limit its lateral motions. Other motion control examples where solid contact is involved include the wafer stopping and positioning operations indicated in Fig. 1. Essentially, a wafer is stopped at a given location and held in contact with the surface by the suction force provided by vacuum ports. Upon removal of the force, the wafer, again floating on the air film, is propelled by air streams in either the same or a different direction. For processes such as serial number identification, the stopped wafer is rotated in place on the air film to a specific position where it is again held, identified, released, and transported out in a given direction. This orienting operation requires considerable positioning accuracy and in the past has been done by techniques involving continuous edge contact. Because of the physical contact entailed in effecting such specific wafer motions, past efforts in developing air film apparatus have sought particular materials and constraint designs to minimize damage. Other efforts have focused on creating supporting motive air films with added motion control capabilities in an attempt to eliminate, or at least decrease, the incidence of wafer contact.

In automated wafer handling apparatus currently used at IBM, a particular construction of surface openings is employed to generate an air film with such control characteristics [1]. In essence, air streams at small inclinations with the surface and issuing from a central row of oriented, louvre-type openings move the wafer linearly. Other air streams from rows of similar openings, directed inward towards the travel direction, are intended to keep the moving wafer centered. This arrangement is reasonably effective in providing control. However, some contact still occurs because of the overriding influence of complex motion instabilities associated with the nature of the air film. Characteristically, both pitching and rolling motions are induced as the film propels the wafer linearly and simultaneously constrains its lateral motion. This behavior is ascribed to the absence of any constraint on wafer motion normal to the louvred surface. Furthermore, these characteristic motions are sensitive to and are augmented by slight misalignments in the surface and/or the air louvre orientations. Another sensitivity is associated with the enclosures placed over the film surfaces for atmospheric control purposes. The film air accumulating in the enclosed volume must be continuously vented at numerous locations and in a smooth, controlled manner. This is difficult to do in practice, and the natural occurrence of small deviations causes flow disturbances within the enclosure which aggravate the above behavior. Consequently, these induced unstable motions tend to counteract the intended lateral constraining effect of the air film, and some contacting occurs.

In addition to the air elements for linear transportation of wafers, air track intersections and orienting components are needed for the other motions indicated in Fig. 1. These components also use louvre-type air openings in particular orientations, and various forms of physical contact are involved in the execution of the required motions. Thus, while this general system represents a considerable advance in automated wafer delivery, some likelihood of wafer damage still exists.

Physical contact in the transportation and positioning of wafers is substantially reduced by the air film system developments described in this paper. Basically, edge contact in all wafer movements is completely eliminated. In stopping operations, wafer surface contact is involved, but under greatly mitigated conditions. The system is based on a supporting air film that embodies the suctiongenerating and flow-redirection actions of two fluid mechanics phenomena. This causes the film to exert, simultaneously, a net attraction force on the wafer in addition to pronounced directed forces acting in the plane of the wafer surface. The overall action of the combination of forces is such that an essentially uniform air film thickness is maintained while constraining wafer motion in directions normal to and parallel to the air film generating surface. Thus, motion instabilities stemming from effects such as enclosure flow disturbances and surface misalignments are more effectively resisted.

The air film is generated by a perforated surface that is implemented in different configurations for accomplishing the basic control functions illustrated in Fig. 3. In contrast to the existing louvre-type system, its operation characteristically involves higher air stream velocities in order to create the film. In one version, higher air supply pressures are required, while in a second version, the flow supply pressures for the two systems are comparable. For linear transportation with either version, the supporting air film propels the wafer essentially parallel to the air track surface, while constraining its lateral and vertical motion. For the intersection and orienting components, the air film acts in conjunction with other control techniques, which also utilize certain aspects of fluid flow phenomena. These techniques, operating synergistically with the controlling characteristics of the air film, provide typical control functions such as: sensing the presence of a wafer entering a given location (e.g., an intersection) and generating a pronounced pressure signal; activation, by this pressure signal, of a means for stopping the wafer without the need of an external vacuum source; and other controls associated generally with centering, rotating, redirecting, and accelerating a wafer on the air film. For the wafer orienting function, positional accuracy is achieved by an arrangement of photo-electronic position-sensing and actuating devices operating in conjunction with certain of the above control techniques.

The following sections describe the underlying fluid mechanics principles and their application to air track, intersection, and orienting components for a wafer delivery system.

#### Basic air film surface

The air film generating surface is described with reference to the track structure shown in Fig. 4. It consists of a bilaterally symmetrical arrangement of flat surfaces sepa-

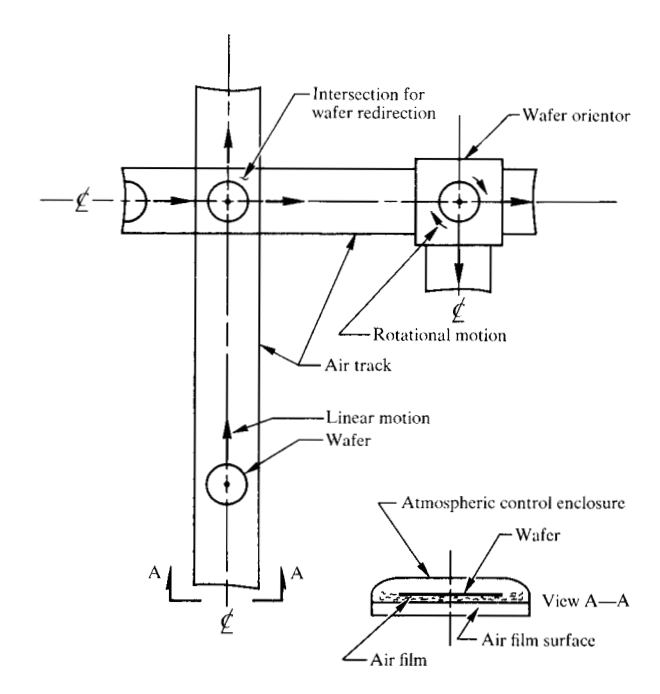


Figure 3 Components of the new air film system.

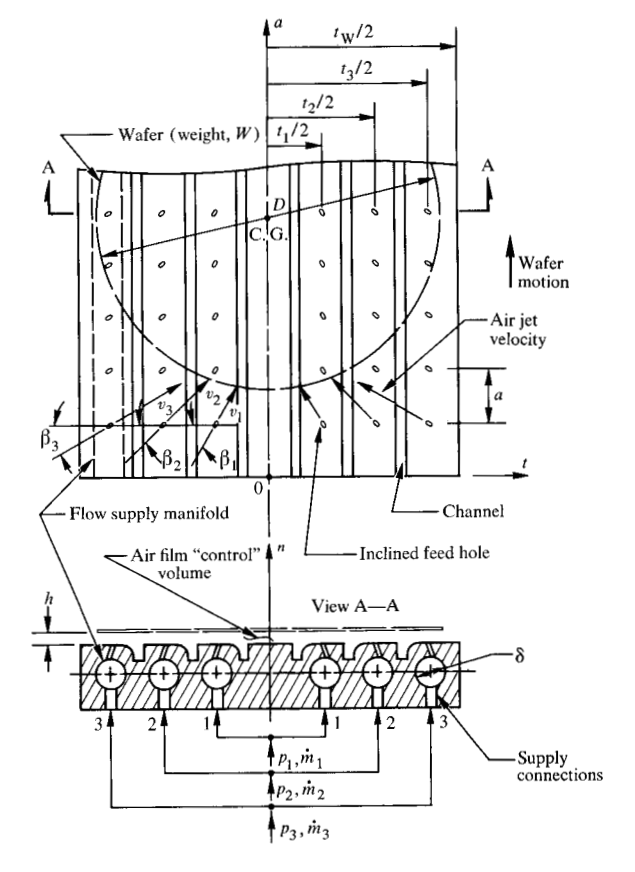


Figure 4 Air track configuration.

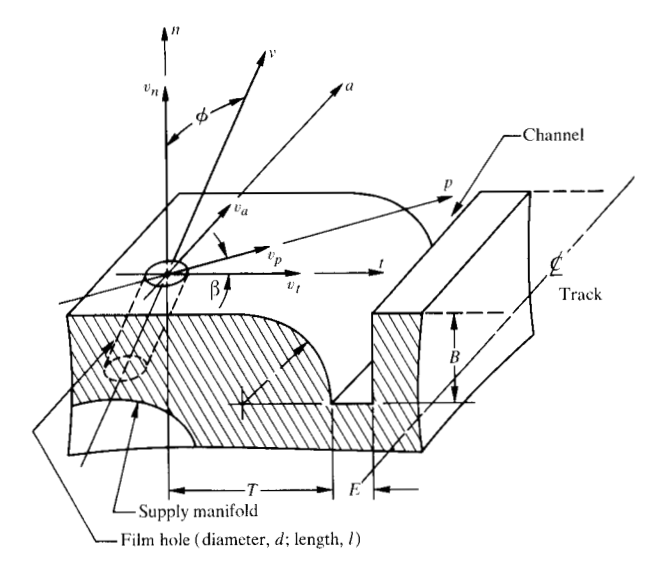


Figure 5 Surface structure parameters.

rated by channels. Each channel has a rounded sidewall which blends tangentially with an adjacent flat region. Air, under pressure in the feed manifolds, is supplied to the surfaces by rows of long holes which terminate in the flat regions in locations essentially midway between bounding channels. These holes are all inclined towards the track centerline at angles  $\phi$  and  $\beta$ , as shown in Fig. 5. Consequently, the velocity v of an air jet issuing from any such hole has components  $v_n$  and  $v_p$  normal to and parallel to the track surface, respectively. The inclination of v for each pair of opposing rows of holes is at a particular set of angles  $\phi$  and  $\beta$ . The variation of this inclination with the hole rows is such that the planar angle  $\beta$  is largest for the innermost rows and smallest for the outermost rows. Thus, as shown in Fig. 4,  $\beta_1 > \beta_2 > \beta_3$  for row pairs 1, 2, and 3, respectively. In addition, the magnitude of the air jet velocity v from each pair of rows is also varied by means of pressure (p)-mass flow rate  $(\dot{m})$  conditions in the appropriate feed manifolds, so that velocity is largest for the outer rows and smallest for the inner rows. Thus, for manifold supply pressure settings  $p_3 > p_2 > p_1$  corresponding to particular air flowrates  $\dot{m}_3 > \dot{m}_2 > \dot{m}_1$ , the relative velocity magnitudes are such that  $v_3 > v_9 > v_1$ . Finally, the track configuration considered here contains air film holes which are all of the same diameter d and of slightly different length l depending on their inclination angles. In another version of the air track, which will be discussed subsequently, the inclined hole diameters for each pair of rows are also varied so that  $d_1 < d_2 < d_3$  for row pairs 1, 2, and 3, respectively. In that configuration, air is supplied to the film holes at the same pressure from a common feed manifold.

By combining the action of two fluid mechanics phenomena, the inclined air jets impinging against the wafer surface produce a supporting air film that exerts multidirectional forces on the wafer. The net attraction force stems from the influence of the suction-generating or Bernoulli flow phenomenon [2, 3]. Here, we call it the "axiradial" effect because of its particular operative flow geometry. As illustrated in Fig. 6, the air jet issuing axially from an inclined hole (Fig. 5) impinges against the wafer surface and abruptly turns to expand in an essentially radial direction. The jet thus produces a flow momentum force in the n direction which acts to overcome weight and repel the wafer from the surface. At the same time, the flow, in turning to expand in the radial direction, separates to some extent from the track surface in the vicinity around the hole. Because of this expansion and separation, a region is created between the wafer and the track surface in which the local static pressure is lower than atmospheric pressure. Downstream from this region, the flow is reattached to the surface, and the pressure increases in accordance with flow behavior in a passage of increasing cross-sectional area. Owing to the relative influence of the suction region, a net attraction force is generated which is sufficient to counteract the effect of the opposing momentum force. Thus, instead of being repelled, the wafer is drawn to and constrained on the air film. As will be discussed subsequently, this overall pressure variation is associated with a complex flow behavior in which both inertia and viscous force effects are present. Characteristically, the radial static pressure variation along the wafer surface is as illustrated by the solid curve in Fig. 6. Because of the hole inclination, the flow separation varies around the film hole region with an accompanying change in the extent and magnitude of the suction effect. Due to the presence of an inherent equilibrating action, the net effect of pressure variation in an angular direction around the hole is to maintain an essentially uniform air film thickness. Any tendency of the wafer surface to tilt is thus continuously counteracted. The attraction force on the entire wafer is provided by the aggregate axi-radial action of the multiple air jets. The resultant flow action produces a uniform air film of a thickness dependent on dynamic force equilibrium conditions that vary with flow supply conditions for a given track geometry.

Both attraction and surface forces on the wafer are enhanced by the "Coanda" effect [4]. This effect, in which a tangentially entering flow smoothly changes direction and follows a curved surface boundary, is implemented by the channel construction in the track surface. Referring to the bottom of Fig. 6, the entering axi-radial streamlines "bend" around the suction region and subsequently become essentially parallel to the flat surface downstream

from the hole. Here they encounter, in part, the effect of the curved surface and turn to follow it. This action extends the suction region as illustrated by the pressure variation curve in Fig. 6. The extension is most pronounced in the direction of the hole inclination  $\beta$ , viz., along the p axis towards the curved surface (Fig. 5). For other radial directions from the hole, this extended effect is diminished and is nonexistent for the exiting radial flow that does not encounter the curved surface. By this basic arrangement, the attraction effect is enhanced, as well as the resultant of the boundary-layer-induced frictional forces acting on the wafer surface in the p direction.

A main reason for the Coanda effectiveness here is the inherent characteristic of the flow to enter the channel in an essentially tangential direction. The induced flow is, in large part, exhausted in axial directions within the channel passage and thus below the plane of the track surface. This action causes a reduction in cross-interference flow effects between opposing film hole rows and thus enhances both the attraction and planar frictional forces acting on the wafer. The resultant surface force action, by the symmetrically opposed rows of air film holes, constrains lateral motion while moving the wafer in an axial direction. Concurrently, the resultant attraction force continuously constrains motion in the normal direction so that the wafer moves essentially parallel to the track surface.

In a sense, the air film produced by the surface (Fig. 4) can be considered as a "control" flow volume comprising an essentially constant film thickness and bounded on either side by the track and wafer surfaces. The force field associated with this control volume produces the wafer motion characteristics described qualitatively above. This force field and hence the motion control effectiveness is, for a given surface geometry, dependent on the inclination (angles  $\phi$  and  $\beta$ ) and flow velocity (v) of the air jets in each pair of opposing film hole rows. A quantitative description of this and other parametric relationships is not tractable owing to the extreme complexities of the overall problem. Consequently, our developments were based largely on experimental studies in conjunction with certain supporting analytical efforts. We proceed with a further discussion of the fluid mechanics structure and performance of the air film by first focusing on characteristics of the axi-radial flow.

#### • Basic aspects of the axi-radial effect

Consider a particular representative flow model of the phenomenon as depicted in Fig. 7. Here, a flat circular disk of diameter D and weight W is supported on an air film of constant thickness h. Perfect radial symmetry is assumed so that no unbalanced horizontal forces exist,

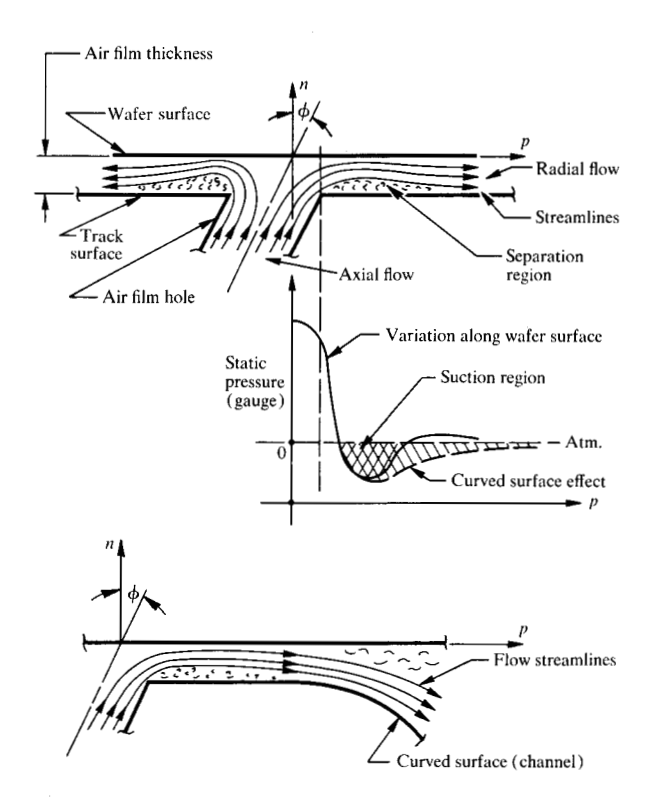


Figure 6 Axi-radial and Coanda flow characteristics.

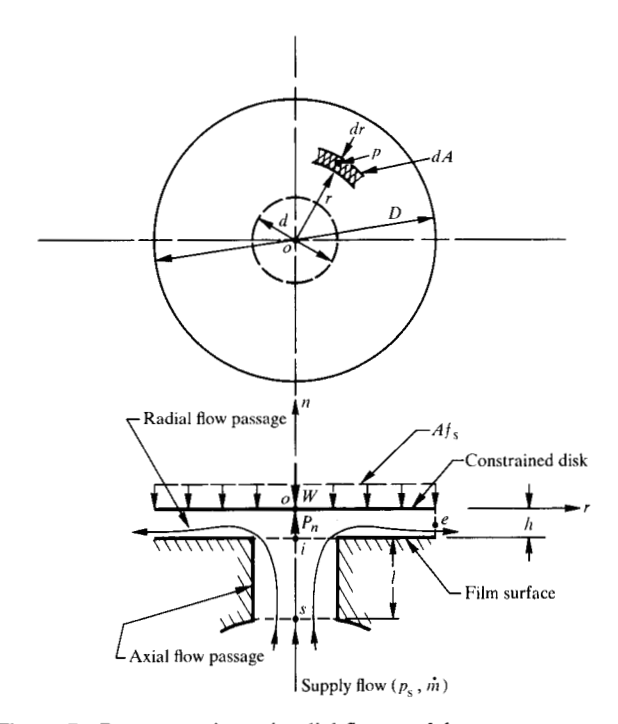


Figure 7 Representative axi-radial flow model.

365

which would cause a corresponding motion of the disk on the low-friction air film. Air at a gauge pressure  $p_{\rm s}$  and steady mass flow rate  $\dot{m}$  is supplied to the film flow passage by a hole of diameter d and length l, perpendicular to the disk. The radial pressure variation along the disk surface reflects the influence of both inertia and viscous forces in the flow. At low Reynolds number viscous flows, the presence of accelerations in the radial inlet region produces significant inertia effects. For the special case of steady, incompressible, and purely radial flow between parallel plates, studies [2, 3, 5] have shown the existence of a depressed pressure region due to these additional effects. For example, the analysis by Livesey [5] provides an approximate radial pressure distribution of the form

$$p_1 - p_2 = \frac{6\mu \dot{m}}{\pi \rho h^3} \ln \frac{r_2}{r_1} - \frac{3\dot{m}^2}{4\pi^2 h^2 \rho} \left( \frac{1}{r_1^2} - \frac{1}{r_2^2} \right), \tag{1}$$

where  $p_1$ ,  $p_2$  are, respectively, the pressures at radial locations  $r_1$ ,  $r_2$ ;  $\rho$  and  $\mu$  are the density and coefficient of viscosity, respectively. The second term on the righthand side represents the pressure change due to inertia effects and is of opposite sign to that of the viscous pressure drop. A depressed pressure region is therefore indicated and, as Livesey shows, the inertia effects are sufficiently large to cause this condition at quite low Reynolds numbers. For the axi-radial flow configuration, this pressure behavior is even more pronounced due to augmentative flow acceleration effects occurring in the inlet region. Thus, even for incompressible viscous flow, as in the present application, the radial pressure variation is of the form illustrated qualitatively in Fig. 6. In the model, this variation is the same in any radial direction because of the axisymmetric flow conditions.

The impinging flow exerts a normal momentum force  $P_n$  acting at the stagnation point at the center o of the disk. Because of the pressure variation, this force is concurrently opposed by an average suction pressure loading  $f_s$  acting over the surface area A of the disk. This results in constrainment of the disk at a given air film thickness h, at which an equilibrium of vertically acting forces exists such that  $P_n - A f_s - W = 0$ . Application of the impulsemomentum principle for steady and assumed one-dimensional flow conditions at the hole inlet (s) and exit (e) regions of the flow passage results in

$$ap_{s} + \frac{\dot{m}^{2}}{\rho a} - 2\pi \int_{0}^{D/2} prdr - W = 0,$$
 (2)

where a is the inlet hole flow area and p is the gauge pressure acting on the disk at r. The forces  $P_n$  and  $A f_s$  are thus

$$P_n = ap_s + \frac{\dot{m}^2}{\rho a} \quad \text{and} \tag{3}$$

$$Af_{\rm s} = 2\pi \int_{0}^{D/2} pr dr. \tag{4}$$

Characteristically, as the supply flow rate is changed, these forces assume different values while their difference remains a constant equal to W [Eq. (2)]. Their individual values at a given flow rate are thus coupled to a particular spacing, h. Consequently, h varies with flow rate in a manner that reflects the relative influence of these forces. A comprehensive theoretical treatment of these characteristics, which are coupled with flow in a passage of variable spacing, is extremely difficult and is not available. Some quantitative estimate of this behavior can be obtained by use of radial static pressure variations such as illustrated by Eq. (1) or improvements to this approximation as given in [3]. However, this approach ignores effects associated with axial flow turning into the radial inlet region. The pressure variation in the vicinity of this region thus differs quantitatively from that predicted by purely radial viscous flow analysis.

The developments described in this paper were undertaken by first conducting preliminary experimental studies of the axi-radial characteristics with appropriate models. With these observations as a guide, air film surface models were developed embodying the axi-radial and Coanda effects. The configurational details and experimentally determined performance characteristics of these surface models are described subsequently. From the initial axi-radial flow studies conducted under laminar flow conditions, it was generally observed that the l/d ratio of the inlet hole (Fig. 7) has an important influence on the flow stability. This influence is evidently related to the socalled hydrodynamic entrance length required for the flow to reach a developed laminar state [6]. The l/d ratio required to achieve this developed state is given by the condition

$$\frac{l}{d} > 0.058R_{\rm e},\tag{5}$$

where  $R_{\rm e}=2\dot{m}/\mu\sqrt{\pi a}$  is the flow Reynolds number. For l/d ratios less than the Eq. (5) condition, the undeveloped flow issuing from the hole at location i has an apparent adverse effect on the suction generation mechanism. We observed that the decreased attraction capability is generally reflected by larger air film thicknesses and by tendencies toward instability or flutter of the constrained disk.

Other studies were made of the effect of hole inclination on the uniformity of air film thickness. We observed essentially uniform thicknesses for inclination angles ranging from zero to approximately 50° with the vertical. This characteristic is evidently due to an inherent equilibrating action associated with the asymmetric pressure

distribution in the air film. For this condition to exist, the resultant moment exerted by the pressure loading must counteract the surface tilting moment due to the action of the normal momentum force.

### • Combination of axi-radial and Coanda effects

Considering a single hole and the adjacent "Coanda" channel (Fig. 5), the combined flow action produces forces on the wafer as illustrated in Fig. 8. The planar force  $P_n$  acting in the direction of the velocity component  $v_n$  (i.e., the p axis) is the resultant of the frictional forces due to the flow boundary layer effect [6]. The variation of the velocity component  $v_n$  with normal distance in the air film is as illustrated for a direction i-i normal to the p axis. The axi-radial flow induced into the channel by the Coanda effect promotes an extension of the suction region (Fig. 6) and increases the magnitude of the velocity gradient at the wafer surface. This action increases flow shear forces and thus the force  $P_p$  is augmented in the pdirection. For the given force  $P_n$ , the extended suction behavior increases the  $Af_s$  force and thus enhances the stability of the air film. The force  $P_p$ , with components  $P_q$ and  $P_i$ , thus imparts motion to the vertically constrained wafer in the axial (a) and transverse (t) directions, respectively. The combined action of the two flow phenomena is effectively achieved for a range of surface configuration dimensions T, R, E, and B (Fig. 5). Basically, for a hole of given l, d, and inclination  $\phi$ , a minimum flat surface region around the hole (e.g., a circular region of radius T – R) is required for the proper development of the axi-radial effect. We have observed that a range of surface areas above this minimum is effective. Similarly, the channel dimensions satisfying given minimum requirements also have a range of values for which the coupled Coanda action is effective. The radius R for given T, E, and B can have different practical values above a minimum for the air track application. For other surface configurations, such as for the intersection and orientor applications, the value of R can be relatively smaller. In a later version of the wafer orientor, which will be described subsequently, a value of  $R \approx 0$  has been found to be practical. In this case, the Coanda effect has been reduced to flow over a "step" region as provided by the channel with vertical sidewalls. Because of the nature of this kind of flow configuration, a part of the directed axi-radial flow is still induced into the channel by attendant expansion effects. While the effect of this action is less than that with a rounded sidewall surface, it still provides a sufficient augmentation of the force  $P_n$  for this particular application.

Referring to Figs. 4 and 9, the above discussion is extended to the air track configuration containing three pairs of symmetrically opposed rows of air film holes. Corresponding to the previously described variation of air

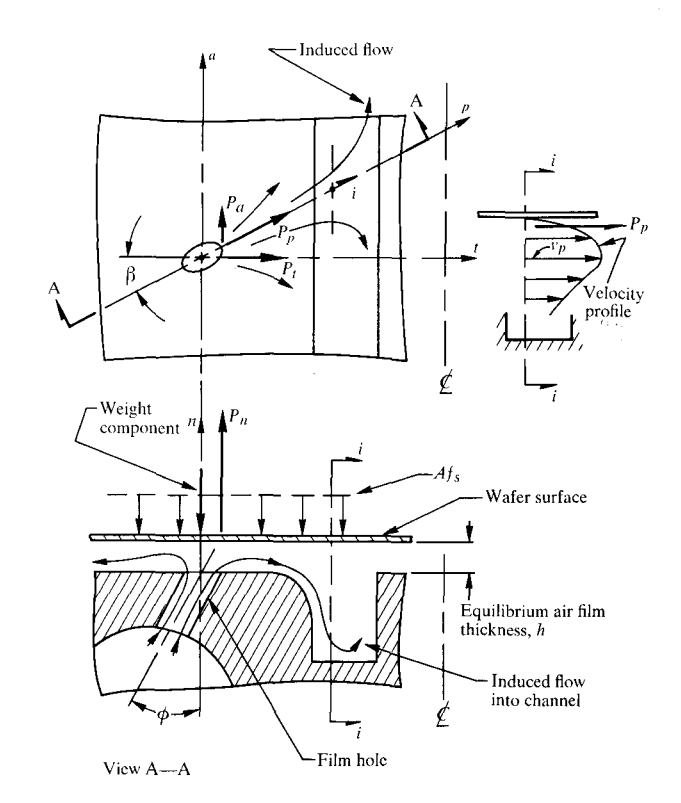


Figure 8 Applied wafer forces due to the combined flow action.

jet velocity, the forces for row pairs 3, 2, and 1 are such that  $P_{p3} > P_{p2} > P_{p1}$  and  $P_{n3} > P_{n2} > P_{n1}$ . The air film "control" volume exerts on the wafer a total normal momentum force equal to  $\Sigma P_n$  and an average attraction force  $F_s = \Sigma A f_s$ . The wafer is thus constrained on the air film of a uniform thickness h in accordance with the extended force equilibrium condition of Eq. (2), viz.

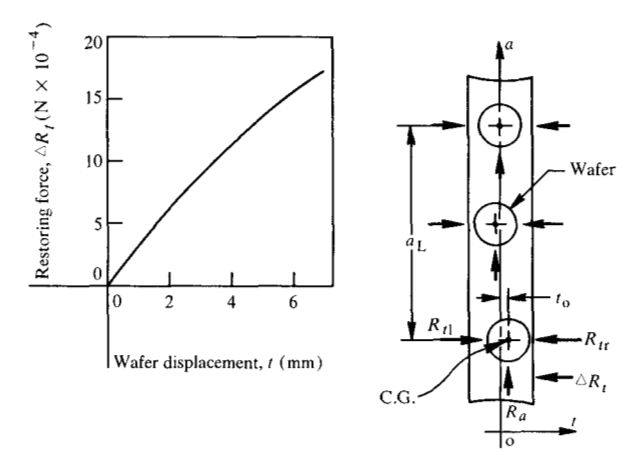
$$\sum P_n - F_s - W = 0. \tag{6}$$

The wafer is given axial motion by a resultant force  $R_a$  equal to the sum of the planar axial force components acting on its surface, viz.

$$R_a = \sum P_a,\tag{7}$$

where  $\Sigma P_a = \Sigma (P_{a1} + P_{a2} + P_{a3})$  and  $P_{a1} > P_{a2} > P_{a3}$ . The oppositely directed transverse force components,  $P_{t1} < P_{t2} < P_{t3}$ , act to keep the moving wafer centered with respect to the track symmetry axis a. When the center of gravity (C. G.) of the wafer is on the a axis, the sum of these forces on the left side of the symmetry axis  $R_{t1}$  is just balanced by the sum of the forces on the right,  $R_{tr}$ . If the wafer C. G. moves in the t direction, an unbalanced force,

$$\Delta R_t = R_{t1} - R_{tr},\tag{8}$$



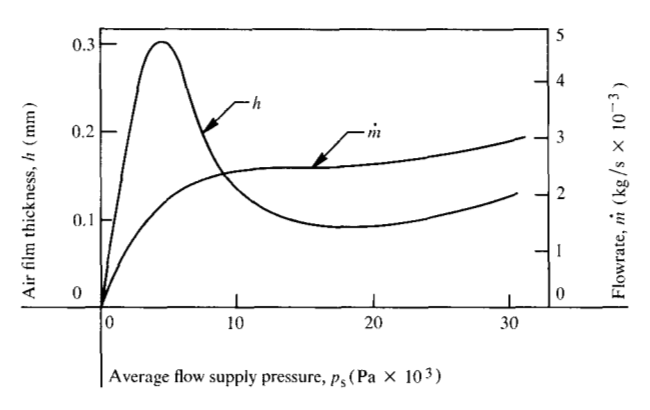


Figure 9 Air track operating performance characteristics.

is created which acts to restore the motion. The  $\Delta R_t$  force increases with displacement in the t direction because of the opposing effect of increasing  $P_t$  forces acting on an increasingly larger part of the displaced wafer surface area. The effectiveness of  $\Delta R_t$  in restoring symmetrical axial motion is enhanced by the implemented variation in the magnitude and direction of the  $P_t$  and  $P_a$  forces in the transverse direction. The overall result of this arrangement is that the generated force field acts not only to effectively restore the desired motion, but also provides a stronger resistance to any initial deviation from this condition.

Some performance characteristics of the track air film are illustrated in Fig. 9. For a given wafer weight W, the variation of h with  $p_s = 1/3(p_1 + p_2 + p_3)$ , while complying with the force equilibrium condition of Eq. (6), is as shown. Due to the intrinsic action of this condition, a variation in W(e.g.), such as would be encountered with wafers in different stages of processing) is reflected by a shift to a different equilibrium value of h. The variation

of  $\dot{m}=\dot{m}_1+\dot{m}_2+\dot{m}_3$  exhibits an appreciable range where it is essentially insensitive to the value of  $p_s$ . This range is coupled to a similar kind of behavior in the variation of h and is a typical characteristic of the axiradial flow action. The flexible vertical constraining property of the air film is thus manifested at an essentially constant h over a given operating range of  $p_s$ . We have observed that the effectiveness of the constraining air film is realized for an appreciable range of supply pressure conditions which, in turn, affords a considerable practical advantage.

The axial velocity of the wafer is controlled by varying  $p_s$  and thus the force  $R_a$  [Eq. (7)]. A wide range of velocity and acceleration conditions is achievable while effectively controlling wafer motion in the normal and transverse directions. With increased  $p_s$ , the planar forces  $R_{t1}$ ,  $R_{tr}$  and therefore  $\Delta R_t$  [Eq. (8)] are enhanced. The typical variation of  $\Delta R_t$  with displacement t of the wafer C. G. from the a axis is as shown in Fig. 9. The variation is approximately linear in a range of practical interest,  $t_r$ , and we define an air film "spring constant" for this range as  $K \approx \Delta R_t/t_r$ . In view of the essentially uniform constraint of wafer motion in the normal direction, the action of  $\Delta R_t$  in restoring symmetrical axial motion is involved with an equation of motion of the general form

$$m\frac{d^2t}{d\tau^2} + c\frac{dt}{d\tau} + Kt = mF(a,\tau), \tag{9}$$

where  $\tau$  denotes time; c, an air film "damping constant"; m, the wafer mass W/g; and F, a function of a and  $\tau$ . The term  $c(dt/d\tau)$  represents the damping force variation with t and  $\tau$ ; and Kt is the restoring force  $\Delta R$ , for the range  $0 \le$  $t \le t_r$ . A wafer moving at a given axial velocity and displaced a distance  $t = t_0$  at time  $\tau = 0$  (see Fig. 9) must recover symmetrical motion (t = 0) in the shortest possible distance  $a_{\rm L}$ . This distance is influenced by momentum of the moving wafer and by the magnitude of  $t_0$ . The decaying oscillatory behavior of t with respect to the a axis is associated with the underdamping condition for which  $c < 2\sqrt{mK}$ . Measurements of c and K were made for various film hole inclination patterns  $(\phi, \beta)$ , in conjunction with different air jet velocity variations (i.e., by adjustment of manifold pressures  $p_1$ ,  $p_2$ , and  $p_3$ ). The basic film hole arrangement and flow supply conditions reflect a maximization of c and K values while complying with the underdamping condition. This results in an enhanced recovery capability and a stronger resistance to deviations from symmetrical motion.

• Air track dimensions and general operating conditions The air track (Fig. 4) was designed to accommodate two wafer sizes at the same operating air supply conditions: viz.,  $D = 82 \text{ mm } (W \approx 5 \text{ g}) \text{ or } D = 57 \text{ mm } (W \approx 2.4 \text{ g})$  wafers. The approximate surface configuration dimensions (Fig. 5) are:  $t_w = 95 \text{ mm}$ , T = 9.5 mm, R = 3.2 mm, E = 1.8 mm, and B = 3.2 mm. With regard to spacing of the air film hole rows, some variation is possible without sensitive influence on the wafer motion. The spacings in the present design are  $t_1 = 22$  mm,  $t_2 = 51$  mm, and  $t_3 =$ 73 mm. Each pair of rows contains air film holes of diameter d = 0.34 mm, and the holes are uniformly spaced at a distance a = 19 mm. The arrangement is such that the holes in each row pair are aligned with respect to the t direction at any axial location a. This location pattern and hole spacing represents one of several different arrangements that were investigated and found to be essentially equally effective. The average length l of all the film holes is approximately 1.8 mm. The film hole length for each pair of rows is slightly different because of the different inclination angles  $\phi$  and  $\beta$ . These angles are:  $\phi_1 = \phi_2 = \phi_3 = \phi_4 = \phi_4 = \phi_5 = \phi_$  $\phi_3 \approx 22^\circ$  and  $\beta_1 \approx 64^\circ$ ,  $\beta_2 \approx 45^\circ$ ,  $\beta_3 \approx 26^\circ$ . Air is supplied to the film holes from internal feed manifolds of diameter  $\delta = 13$  mm. The supply pressures  $p_1 < p_2 < p_3$  for the row pairs are set by using the corresponding stagnation pressures of the issuing air jets as the basic indicator. For example, the pressure  $p_1$ , and hence the flowrate  $\dot{m}_1$ , is set by placing a manometer total pressure tube over a given film hole. The desired stagnation pressure is then obtained by adjustment of the value  $p_1$ . We observed that the stagnation pressure settings can be varied over an appreciable practical range without adverse effect on performance. Typical operating settings for row pairs 1, 2, and 3 are, respectively: 125, 375, and 750 mm of manometer water column. For this condition, the approximate average supply pressure,  $p_s = 1/3 (p_1 + p_2 + p_3)$ , is  $11 \times 10^3$ Pa; and the corresponding mass flowrate,  $\dot{m} = \dot{m}_1 + \dot{m}_2 +$  $\dot{m}_{\rm a}$ , per meter of track length is approximately 2.5  $\times$  $10^{-3}$  kg/s. The air supply connections to the manifolds are located at track length intervals of approximately 6 meters. Because of flow pressure drop, the above stagnation pressure values, adjusted at a given transverse location, vary with axial distance along the track. Due to the flow resistance characteristics of the rows of small film holes, these pressures decrease in an approximately linear manner and at essentially the same rate. Consequently, the maximum stagnation pressure decrease for a track length of 6 m is approximately 30 mm water column for each of the above settings. The performance of the air film is essentially unaffected by this decrease in the pressures.

The track configuration is constructed from aluminum in a width larger than  $t_{\rm w}$  in order to accommodate a plastic cover for atmospheric control purposes (see Fig. 3). Thus, the overall width is 133 mm and its thickness is 21 mm. The entire configuration is constructed by an extrusion process in track lengths of approximately 2 meters. Following a surface smoothing machining operation,

the film holes are drilled in the structure. Satisfactory track operation does not require an overly sensitive horizontal alignment of its surface. For example, surface deviations of approximately 0.1° from the horizontal do not adversely affect the control capability of the air film. In operation, dry filtered air is supplied to the covered track at axial intervals as noted above. The air accumulating in the enclosure, at a pressure slightly higher than atmospheric, is vented at various axial locations on the cover. An important characteristic of the air film is that its control effectiveness is not reduced by irregularities in the venting operation. Thus, venting requirements are not stringent. With regard to motion stability characteristics, measurements of c and K [Eq. (9)] were made for both wafer sizes under various velocity and displacement conditions. For a typical operating velocity of 0.5 m/s and an extreme displacement  $t_0 = 1/2 (t_w - D)$ , the recovery distance  $a_1$  for both sizes was less than 1.2 meters (Fig. 9). For smaller values of  $t_0$  and/or axial velocity, the recovery distance  $a_1$  was reduced. On the other hand, for a velocity greater than the above value, say 1.0 m/s, and for displacements  $t_0$  of the order of 1/4  $(t_W - D)$ , recovery also occurred in a distance less than 1.2 meters for both wafer cases. For the above flow supply conditions, the average damping and spring constants indicated for either wafer size are on the order of  $c \approx 0.018$  N/m/s and  $K \approx$ 0.27 N/m. Typical equilibrium air film thicknesses h for the above operating conditions are on the order of 0.1 mm.

As noted previously, another version of the air track was developed in which air is supplied to the film holes at a reduced and common pressure  $p = p_1 = p_2 = p_3$ . The purpose of this effort was to extend application of the track to very low operating pressure conditions, such as those associated with blower air supply equipment. This equipment is used in operation of the existent louvred system discussed previously. The configuration and dimensions of this version of the track are the same as those described above, with the exceptions of the air supply arrangement and the film hole aspects. Basically, in order to obtain the low operating pressure conditions, larger diameter (d) film holes are used with an average length (l) approximately the same as for the above track. In view of this construction, the l/d ratio of the holes is somewhat less than  $0.058R_{\rm e}$  [see Eq. (5)]; consequently, this condition reduces the axi-radial flow action to some extent. To compensate for this the film hole diameters are varied so that  $d_1 < d_2 < d_3$  for row pairs 1, 2, and 3, respectively. In addition, the corresponding angles  $\beta_1$ ,  $\beta_2$ , and  $\beta_3$  are increased for the same angle  $\phi$  as in the above track. By this configuration, the flowrates  $\dot{m}_1$ ,  $\dot{m}_2$ ,  $\dot{m}_3$  at the common supply pressure p are distributed in a way which compensates for the effect of reducing the l/d ratio of the

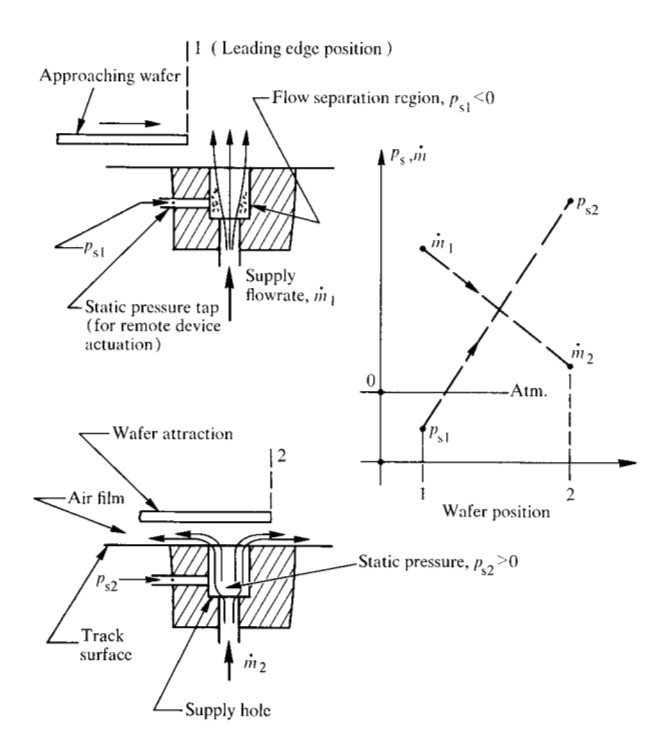


Figure 10 Axi-radial sensor operating principle.

holes. The film hole diameters and inclination angles are:  $d_1 = 0.4$  mm,  $d_2 = 0.7$  mm,  $d_3 = 0.9$  mm, and  $\beta_1 \approx 72^\circ$ ,  $\beta_2 \approx 55^\circ$ ,  $\beta_3 \approx 32^\circ$ , where  $\phi \approx 22^\circ$  for all the holes. Because of reduced pressure drop effects, the air feed to the film holes requires supply connections at track length intervals of approximately 2 m instead of 6 m, as in the previous case. Typical operating conditions for the track are  $p \approx 150$  mm of water column and  $\dot{m} = \dot{m}_1 + \dot{m}_2 + \dot{m}_3 \approx 6 \times 10^{-3}$  kg/s per meter of track length. The corresponding equilibrium air film thickness h associated with the condition of Eq. (6) is approximately 0.15 mm. The performance characteristics of this version of the track are similar to, but quantitatively less effective than, those for the other track. However, this situation is not appreciable from a practical standpoint, and satisfactory performance for either size wafer is still obtained.

#### Wafer motion control techniques

As indicated previously, the basic film surface is implemented in different constructions for accomplishing the wafer motion functions illustrated in Fig. 3. In the performance of these functions, the air film acts in conjunction with other evolved control techniques, as described below.

## • Position sense and signal generation

This technique utilizes a particular aspect of the axi-radial effect to detect a wafer moving over a given location on

the air film. The presence of a wafer is manifested as an abrupt pressure increase, which is used to actuate a control device to be described subsequently. Its basic operation is illustrated by means of Fig. 10, which shows a hole located normal to and terminating in a flat part of the film surface. Air is supplied to the hole from a source separate from that supplying the air film holes. The air jet at a mass flowrate  $\dot{m}_1$  and an upstream pressure  $p_{s1}$  issues from the surface at a velocity greater than that from the surrounding air film holes. As the leading edge of the moving wafer passes over the jet, an abrupt suction region is created which, in turn, abruptly increases the pressure to  $p_{s2}$ while the flowrate decreases to  $\dot{m}_{2}$ . By nature, this flow action operates synergistically with the air film characteristics; hence, its control capabilities are not disrupted by the generated additional suction effect. This technique is highly effective for a broad range of sensor hole dimensions and flow supply conditions. In the present application, a length-to-diameter ratio of approximately 8 is used with a hole diameter of 1.0 mm. In operation, the supply flowrate at  $\dot{m}_1$  is adjusted so as to obtain the required resulting pressure  $p_{s2}$ . As illustrated in Fig. 10, the sensor hole is fed from a relatively smaller diameter hole; e.g., approximately 2/3 that of the sensor hole. Thus, the operating pressure  $p_{s1}$  is always maintained at or somewhat below atmospheric. Typical operating values of  $p_{s2}$ are on the order of  $14 \times 10^3$  Pa and are generated over time intervals on the order of 0.1 to 0.2 second.

#### • Stop technique

A wafer moving on the air film is stopped at a given location by a technique which utilizes the aspiration property of an air jet [6]. The implementation of this technique is illustrated by the air track arrangement in Fig. 11. Here, air jets are positioned so that they issue in a direction parallel to and along the lower or floor region of the channel. Because of the localized entrainment action, air is aspired down into the channel and carried away by the jet streams. This behavior manifests itself as a generated suction effect which is most intense at the jet exit region and gradually decays in a downstream direction due to the increasing entrainment of air. As in the case of the sensor technique, these jets are fed from a separate air source. The wafer, moving on the air film over a location containing these jet devices, is stopped by initiating this air jet action. The ensuing suction effect strongly aspires the air film into the localized channel regions, which results in the stopping and constraining of the wafer at the given location.

Characteristically, this stopping action occurs abruptly but uniformly and is achieved by using an appropriate distribution of air jet devices at the location. The stopping process may or may not involve planar contact between the wafer and the film surface structure. In one set of conditions, stopping takes place on a squeezed, much reduced, air film thickness separating the two surfaces. At higher aspiration power (i.e., with increased air jet flow) and other conditions equal, the film thickness becomes vanishingly small and light surface contact ultimately occurs. Typical air jet hole constructions are approximately 3.5 mm long with a cross-sectional area of  $30 \times 10^{-8}$  m<sup>2</sup>. Air is supplied to the aspirator jet devices at pressures on the order of  $20 \times 10^3$  Pa. The desired aspiration effect is fairly insensitive to minor variations in the supply pressure. Thus, the operating pressure adjustment is a simple procedure.

In the wafer sense-stop operation illustrated by Fig. 11, the leading edge of the moving wafer passes over the axiradial sensor which abruptly generates a pressure  $p_{\rm s2}$  (Fig. 10). This pressure activates a flow supply to the aspirator jets which results in stopping of the wafer. When the flow supply to the sensor is turned off,  $p_{\rm s2}$  is reduced to zero and the flow supply to the aspirator jets is turned off. The wafer is thus released and proceeds to move along the track by the action of the inclined air film holes. This basic operation is applied in different forms with other techniques in the intersection and orientor control functions, as will be described subsequently.

#### • Other motion control aspects

Controlled axial motion on the track is provided by the inclined air film holes, as explained previously. In addition, pairs of inclined air jets fed from a separate air source are used at given locations in order to obtain specific motion control. Basically, these additional jets, which also utilize the axi-radial effect, redirect and/or accelerate wafer motion (e.g.), as at an intersection). Hole dimensions and inclination angles are about the same as in the case of the film holes. Various arrangements and sizes can be used to achieve specific motion control in given axial, radial, or rotational directions.

For wafer rotation, while maintaining normal and radial direction constraint (viz., an orientor requirement), tangentially directed and opposing pairs of these jets impart the desired motion control. As in the case of the axi-radial sensor, the action of these additional "driver" jets complements the characteristics of the air film. Thus, stable motion control is continuously maintained. In addition to these control aspects, arrangements of extra air film holes operating in a different manner are used in the intersection and orientor components. Basically, their use is associated with enhancing the operation of symmetrically positioning a wafer on the air film of these components. For this purpose, these additional holes are inclined and distributed on a circle concentric with and of a diameter

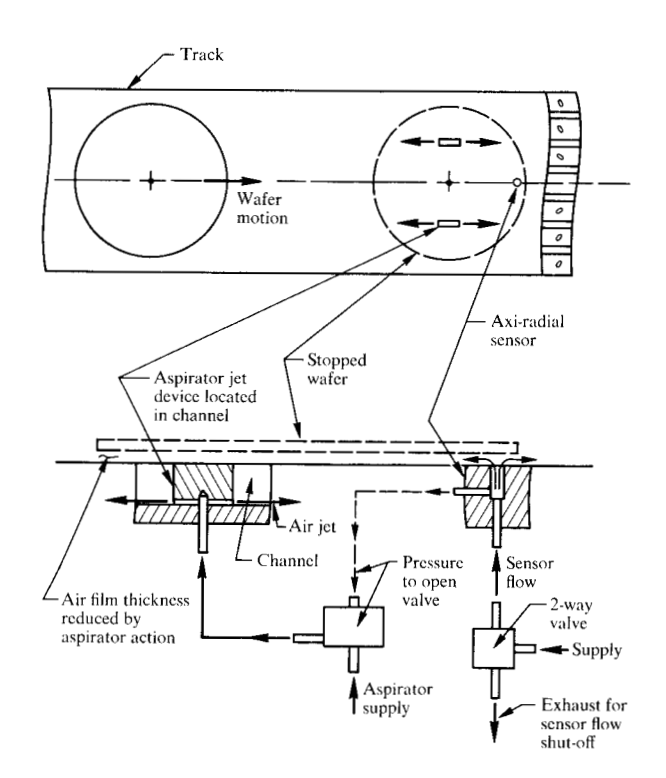


Figure 11 Illustration of the air jet aspirator technique for stopping a wafer.

slightly larger than that of the wafer located in a centered position. The action of these "peripheral" air jets both accelerates centering of the wafer and enhances its constrainment in the symmetry position. Once the wafer is in this position, it is subsequently accelerated out in a particular direction by a pair of driver jets at a given adjusted velocity (viz., the intersection function). Alternatively, as a part of the specialized orienting function, the centered wafer is rotated in place on the air film by tangentially directed driver jets as described above. Upon completion of the other aspects of this function, the wafer is accelerated out as in the case of the intersection.

Finally, it is again noted for general emphasis that in the basic action of these driver and peripheral jet arrangements, the inherent controlling characteristics of the air film are predominant in maintaining stable motion. This has been observed to be the case for a wide variety of such arrangements. As an extreme example, a wafer moving along an air track can be decelerated by pairs of driver jets inclined against the direction of motion. By placement of these jets at particular locations along the track, deceleration is accomplished while the air film maintains a continuous and uniform constraint of the motion in the vertical and horizontal directions.

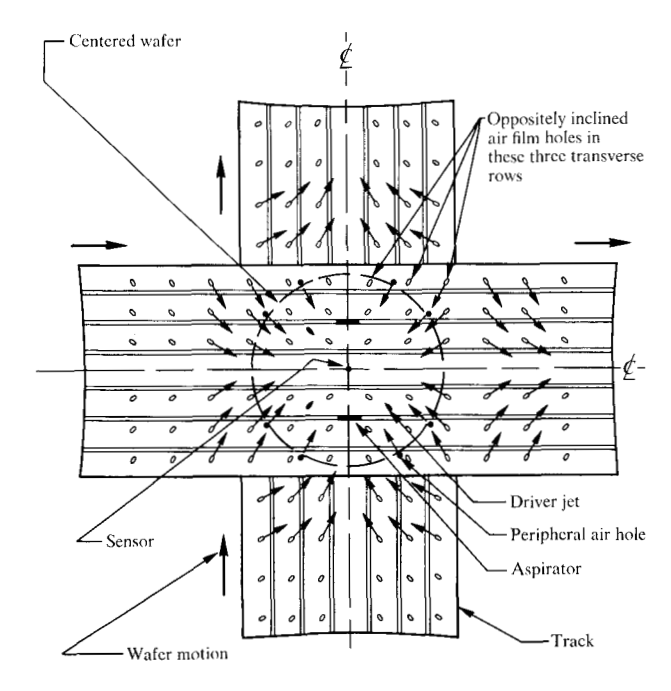


Figure 12 One configuration of the air track intersection.

#### • Air track intersection

One configuration of the intersection component for performing the wafer control function illustrated in Fig. 3 is shown in Fig. 12. The component utilizes the track structure and is equipped with the above control techniques consisting of an axi-radial sensor and an arrangement of driver, peripheral film hole, and aspirator air jets. In addition, the intersection region contains three pairs of transverse rows of air film holes which are opposed in a symmetrical pattern. All the hole sizes, spacing dimensions, hole inclination angles, and flow supply conditions are as described previously for the track (Fig. 4). By opposing the holes in this manner, the air film constrains the wafer in the position indicated. The peripherally located air film holes are placed along a circle of a diameter  $D' \approx D + 2d$ . The three driver air jet holes, of diameter 0.4 mm and 6 mm in length, are symmetrically arranged with respect to the intersection center and are spaced at a distance of approximately 32 mm apart. Their inclination angles are all the same, viz.,  $\beta = 45^{\circ}$  and  $\phi \approx 22^{\circ}$ . These jets are implemented in the track by means of separate, inserted devices. The flow supply arrangement is such that the middle device operates with either one of the other two devices. Thus, two independently controlled pairs of driver jets are provided. The sensor dimensions are as given above, and the aspirator devices inserted in the middle channels (see Fig. 11) are 10 mm long and have the hole dimensions given above.

The motion control function of the intersection is illustrated by means of Fig. 13. The wafer enters the intersection region from either of two directions. As it passes over the sensor jet, the aspirators are actuated and the wafer is stopped in an asymmetric position. The suction effect of one aspirator device is sufficient to cause this action, as illustrated for the case of the wafer entering in the lateral direction. For either entrance condition, when the sensor, and therefore the aspirators, are turned off, the wafer continues into the intersection area. By turning the sensor on and off, the corresponding intermittent operation of the aspirators causes the wafer to move toward the symmetry position in a series of steps. In general, after three or four such aspirator pulses, at time intervals of approximately 0.2 second, the wafer is located in the centered position where it is constrained by the air film. In practice, the pulsing operation is performed automatically by an adjustable electronic device which produces the required flow interruptions. In this application, the device, which can be adjusted with respect to on-off time intervals as well as number of flow interruptions, is actuated by the sensor pressure  $p_{so}$  generated when the wafer is initially stopped at an off-center position. Thereafter, the sensor flow is turned on and off until the centering operation is accomplished. Once centered, the wafer is accelerated out in either of the two directions by actuation of driver jets 1 and 2 or jets 2 and 3. In this operation, the aspirators are actuated to hold the wafer in the centered position, while the pair of driver jets is turned on. When the aspirators are turned off by interrupting the sensor flow, the driver jets propel the wafer out on the track air film. As an alternative procedure, the aspirators are not turned on and the wafer, constrained by the air film, is moved out by simply activating the appropriate pair of driver jets. In either case, the acceleration of the propelled wafer can be varied by adjusting the supply flow to these jets.

The intersection can accommodate the two wafer sizes noted previously. For the smaller wafer, a second circle of peripheral film holes (not shown) of a diameter  $D' \approx$ D + 2d is also included. Otherwise, all the other features and operations as discussed apply to this wafer size as well. Apart from the film and peripheral hole pattern shown in Fig. 12, other patterns have been investigated and found to be of comparable effectiveness. For example, in one such intersection model, just three concentric circles of holes are used where the holes in each circle have a particular set of optimized  $\phi$  and  $\beta$  inclination angles, and the diameters D' of the two larger circles are such that both wafer sizes can be accommodated. Thus, transverse rows of film holes are eliminated, and the total number of holes at the intersection is decreased. Finally, these intersection developments based on the air

track structure of Fig. 4 pertain also to the second version of this track which was described previously. Thus, corresponding versions of intersections, in which the air film holes are supplied at the same air pressure, have also been developed.

Another type of intersection was also developed which subsequently formed the basis for the new orientor component illustrated in Fig. 14. The basic air film surface in this intersection is implemented as a symmetrical configuration with respect to the intersection axes. Air film holes of the same dimensions and spaced approximately as in the air track are all inclined at the same  $\phi$  and  $\beta$  angles in the direction of the center; viz.,  $\phi \approx 22^{\circ}$  and  $\beta \approx 26^{\circ}$ . All holes are fed at the same supply pressure of approximately 150 mm of water column. Their arrangement is such that for either size wafer in the centered position some of the film holes are always located around the wafer periphery to enhance stability. The centrally located aspirator embodies four air jets as shown. The driver jets have the same dimensions and locations as in the previous type of intersection. The operation of this type of intersection equipped with an axi-radial sensor (not shown) is identical to that described above. Finally, as discussed earlier with regard to the general film surface features and dimensions, the radius of the Coanda channel surface in the intersection (and orientor) can be essentially zero without adverse effect on performance.

#### ■ Wafer orientor

In the orientor component based on the above intersection configuration (Fig. 14), the axi-radial sensor is not used; the wafer position sense and aspirator control functions are performed instead by a photo-electronic device arrangement. Two rotation-causing jets are used at each radial location with inclination angles  $\beta = 0^{\circ}$  and  $\phi \approx 22^{\circ}$ . These jets are of essentially the same dimensions as the film holes and are also fed (here) by the air film supply. The optics of the control device consists of two sets of "rough" and "fine" diodes. These diodes sense the edge as well as the notch in the wafer. The diodes, mounted in a control arm as shown, are all exposed to light from sources located in the intersection. When the wafer enters the intersection, in any rotational position, it passes under the control arm and comes in between the diode sets and the light sources. When the light to diode a is blocked off, control circuits actuate the aspirator flow, thus stopping the wafer in an off-center position. Subsequently, the aspirator pulsing operation is applied automatically to center the wafer at the intersection. When this step is accomplished, the aspirator is turned off and the wafer rotates in place until its notch passes under the rough orienting set of the five diodes. The sensing of light by diode c, while an outer diode d is still blocked from the

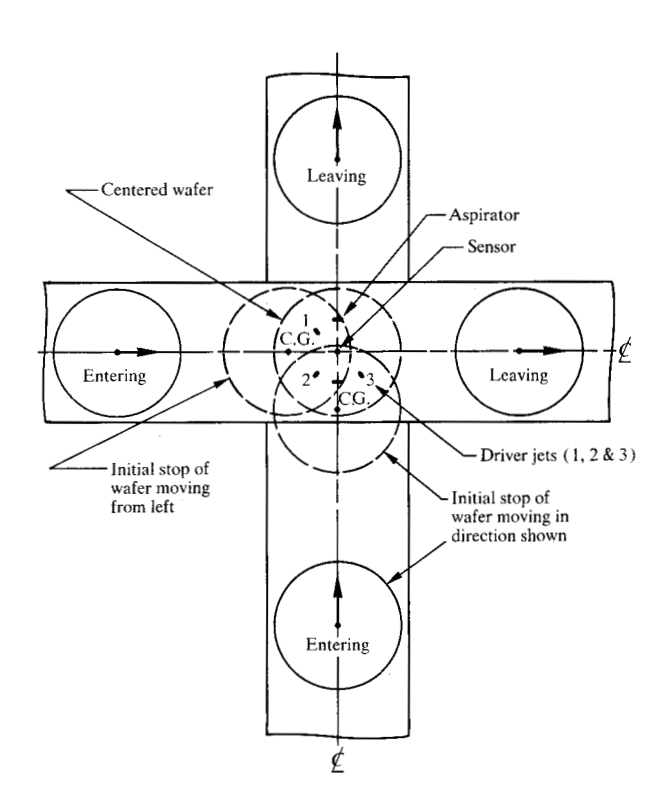


Figure 13 Intersection operation.

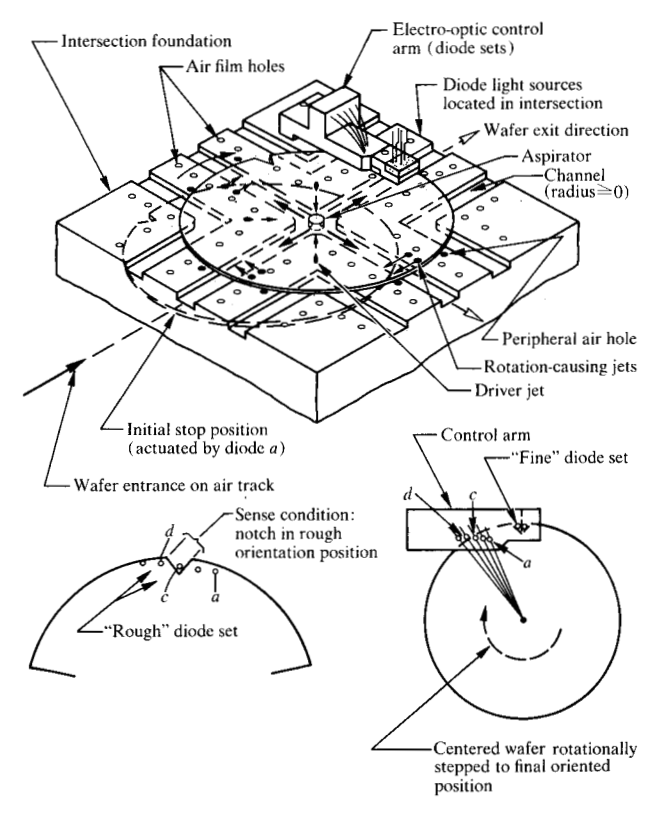


Figure 14 Wafer orientor and operating principles.

light source by the wafer, indicates that the notch is in the rough orientation position. When this happens, control circuits actuate the aspirator pulsing action to rotationally step the wafer to the fine set of two diodes. When both these diodes are exposed to light through the notch, the wafer is in the oriented position and the aspirator stays on, thus holding it in place. Operations such as serial number readings are then performed, and subsequently the aspirator is turned off and the wafer is moved out on the air track by driver jets. This describes the basic motion control operation.

In one variation of this operation, to further enhance the controlling characteristics, the aspirator flow supply is coupled to that of the film holes in such a way that when the aspirator is actuated, the film hole flow is turned off. Thus, during pulsing, mitigated surface contacting occurs due to the cushioning effect of the momentarily interrupted film hole flow. In the oriented position, the wafer is held in direct contact with the film surface by the continuous aspirator action. Since this step involves no relative motion between the surfaces, deleterious effects due to contact are essentially eliminated. The aspirator pulsing action, involving a particular pattern of small and variable time intervals, is such that the overall orienting operation is performed in 10 to 12 seconds. This time period can be varied to some extent by adjusting the flow supply conditions. Finally, the inherent orienting precision of this technique is better than  $\pm 0.04$  mm with respect to the horizontal and vertical directions in the fine diode set region.

The basic orientor construction described above is for a wafer of a particular size as related to the location of the diode-light source system. An orientor having a dual wafer size capability can also be constructed in which the latter system is provided with a location indexing capability. In connection with other configurational aspects, wafer orientor constructions can also be based on the above air track type intersections, as well as on variations of the surface structure in Fig. 14. As one example of the latter situation, a later version of the orientor incorporates essentially only the center channels in conjunction with a smaller number of air film holes. In this design, the diode and light source locations are reversed. As another example of this, orientors have been constructed elsewhere in IBM which use a sharp edge channel construction in a Y configuration. In this design, both symmetrically located aspirator and vacuum pump devices have been investigated for the wafer stopping function. The vacuum pump device is essentially as effective as the aspirator; however, more operational complexity is involved with its use.

#### Discussion and conclusions

The air film system developments described here provide an effective means for accomplishing complex handling functions in an automated wafer delivery system under practically contactless conditions. Motion instabilities and solid contacting of wafers are essentially eliminated. Its constituent air track, intersection, and orientor components feature simple low cost construction and installation advantages. This is exemplified by the extruded aluminum air track construction. The surface machining and hole drilling operations are readily performed by essentially standard techniques. Thus, the cost per unit length of track is lower than that for the existing air louvre system. Because of its simple and robust construction, the system can be readily implemented in various lengths and arrangements. Since its operation is relatively less sensitive to horizontal alignment, installation and subsequent maintainability requirements are facilitated. The low pressure compressed air supply requirements of the system are moderate. However, higher supply flow pressures are required relative to that for the louvre system. In the version of the system which operates with blower air supply equipment, the pressure-flow operating conditions are comparable. The performance capabilities of this latter version are somewhat reduced; however, this is not appreciable from a practical standpoint, and controlled, stable wafer motion is continuously provided. Tests on both versions of the system have indicated a wafer contamination control effectiveness equivalent to that of the louvre system.

The basic air film generated by the combined axi-radial and Coanda effects embodies a unique capability to uniformly control wafer motion in the vertical and horizontal directions. This control is intrinsically flexible; hence, variations, such as in wafer weight and/or in surface texture, are smoothly accommodated. Furthermore, the system resists wafer motion instabilities. When these conditions do tend to occur, its damping characteristics rapidly restore the desired motion control. The Coanda channels greatly reduce cross-interference flow effects between film holes and thus augment the coacting planar and attraction forces on the wafer. If the channels were not present, with other conditions equal, the cross flow effects would greatly reduce these forces and thus the control capabilities of the film would be much less.

The present developments can readily be extended to handle wafers larger than the present sizes. For example, track models have been constructed for 127 mm and 101 mm diameter wafers. In particular, a "universal" air track model has been designed in which the number and arrangement of the air film hole rows and channels are such that all four wafer sizes can be accommodated at the

same flow supply conditions. Furthermore, the present intersection and orientor developments can be readily extended to accommodate these larger wafer sizes.

At this time, a number of orientors, intersections, and a quantity of air track are in use at various locations in IBM.

# **Acknowledgments**

The contributions of R. L. Judge and A. Wutka are acknowledged for their conception of the photo-electronic device system, and for their efforts in the development of the wafer orientor. Thanks are also due to B. W. Reynolds for his assistance in various aspects of the system development. Finally, the extremely helpful discussions with F. Hendriks are appreciated.

#### References

- 1. J. P. Babinski, B. I. Bertelsen, K. H. Raacke, V. H. Sirgo, and C. J. Townsend, U.S. Patent 3,976,330, 1976.
- W. A. Gross, Gas Film Lubrication, John Wiley & Sons, Inc., New York, 1962.
- J. D. Jackson and G. R. Symmons, Appl. Sci. Res. A 15, 59-75 (1965).
- 4. E. K. Parks and R. E. Petersen, AIAA J. 6, 4-7 (1967).
- 5. J. L. Livesey, Int. J. Mech. Sci. 1, 84-88 (1959).
- H. Schlichting, Boundary Layer Theory, Sixth Edition, McGraw-Hill Book Co., Inc., New York, 1968.

Received January 11, 1979; revised March 8, 1979

The authors are located at the IBM Data Systems Division laboratory, East Fishkill (Hopewell Junction), New York 12533.